8/4/98

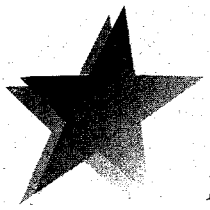

NORTH STAR
RESEARCH CORPORATION

DOE/ER/61935--T1

Final Report: Medical Waste Irradiation Study

R. J. Adler, J. Stein

North Star Research Corporation

J. Nygard,

Advance Bio-Control

Work Supported by DOE under Grant DE-FG03-94ER61935

NORTH STAR 4421 McLeod Rd. NE, Suite A, Albuquerque New Mexico 87109 USA ★ 505.888-4908
FAX 505.888-0072 ★ e-mail 73764.227@compuserve.com

DISCLAIMER

Table of Contents

1.0 Introduction

The North Star Research Corporation Medical Waste project is described in this report, with details of design, construction, operation, and results to date. The project began with preliminary design of the accelerator. The initial design was for a single accelerator chamber with a vacuum tube cavity driver built into the chamber itself, rather than using a commercial tube separate from the RF accelerator. We believed that this would provide more adjustability and permit better coupling to be obtained. We did not have sufficient success with that approach, and finally completed the project using a DC accelerator with a unique new scanning system to irradiate the waste.

2.0 RF Accelerator I

2.1 Chamber

The first RF accelerator chamber designed and built for this project is shown in Figure 1. This chamber is cylindrical in form, about 15-1/2" long and about 19-5/8" in diameter. An axial cylindrical electrode is mounted on each end plate of the chamber, with a 5.6" spacing between the electrode faces with the system assembled. These dimensions provide for a resonant frequency of about 300 Mhz. The chamber and both electrodes are made of 304SS plated with at least 0.002" of bright acid dip copper for good surface conductivity. Two 2" diameter ports (NW50 flanges) are provided in the side of the chamber for instrumentation. A 3" x 9" rectangular port is provided in the chamber wall with its long axis parallel to the chamber axis for mounting the RF excitation "tube" on the chamber. A 6-inch diameter opening is provided in one end face of the chamber for the high vacuum pumping system. One end of the chamber is separable, and is made from an ISO NW500 flange. This flange is secured to the chamber by means of standard claw-clamps, and the vacuum seal is provided by a standard Viton O-ring and aluminum O-ring retainer.

The two electrodes are each about 6" in diameter and effectively 5" long. These electrodes are bolted to their respective end flanges so as to make connection between the copper plating of the electrode and the copper plating of the end flange. Each electrode provides an axial tubular aperture for diagnostics or beam handling. One electrode has this central tube extended out beyond the end flange of the chamber and terminated in an ISO NW50 for beam extraction if desired. The other electrode is mounted on the inside of the other chamber end flange and surrounds a 6-inch diameter vacuum pumping port. This electrode is slotted to permit adequate vacuum pumping speed even if its central aperture is filled with a cathode or other piece of apparatus. A pumping tee is attached to the outside of this end flange.

Q measurements on this chamber were made initially about 3/29/95, and the Q was found to be between 5000 to 6800. We tried making the same measurements again with the end flange not tightly clamped and got Q values of around 2700; on tightly clamping the flange, we got Q values of about 6000. A decision was made to use as few joints as possible in the next iteration of the system.

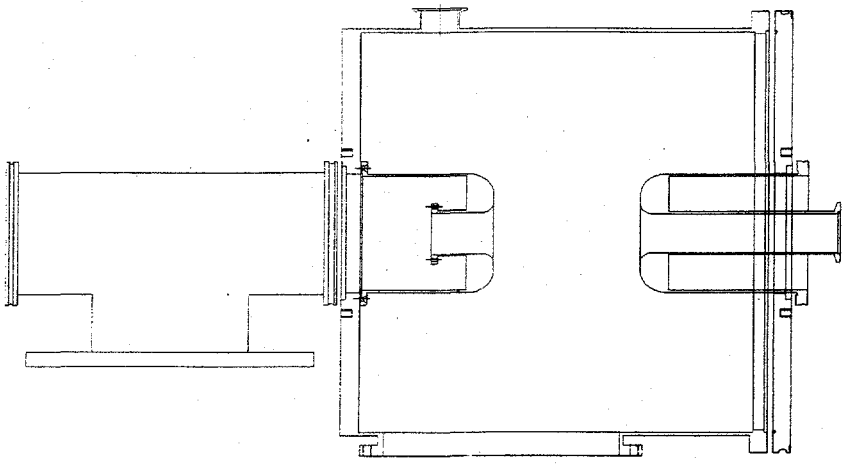

Figure 1 Side view of cavity without the tube section (bottom flange).

2.2 RF Drive System

Figure 2 shows a block diagram of the RF drive system, presently being operated at about 300 Mhz, the approximate resonant frequency of the RF cavity. The RF source is an HP 8654A whose output is gated into 40 microsecond pulses by means of a pulse generator driving a coaxial switch in line with the oscillator output. The output of this switch undergoes amplification by means of several RF amplifiers, the last and most powerful of which can put out a 30 kW RF signal into 50 ohms. A calibrated directional coupler at the output of the 150 W amplifier and another at the output of the 30 kW amplifier provide pickoff points for examining the waveform and also for determining the power level at those points.

The cathode is normally biased positive relative to the grounded grid by 100 volts in order to suppress electron emission between cathode pulses. This DC bias is variable up to 500 volts. When emission is desired, the cathode is pulsed strongly negative in synchrony with the pulse output of the RF power output system. The negative pulse applied to the cathode is continuously variable to a magnitude of approximately 3000 volts. The magnitude of this voltage is the primary determinant of the current in the tube, modulated by the superposed RF pulse applied to the cathode. The anode of the RF system drive tube is maintained positive, up to at least the design level of 25 kV. This voltage is continuously variable.

2.3 Tube

RF drive power is applied to the cavity by means of a demountable grounded-grid triode mounted in the rectangular aperture provided for this purpose in the side of the chamber. A side view of this tube is shown in Figure 3. On the right side is the anode power input and tuning section, which can operate at up to about 25 kV plate voltage. The anode potential is provided by a Plastic Capacitors solid state supply, controlled by a Variac. The solid copper anode itself is seen at the top of the figure, extending from the anode feed section on the right over to the left to face the cathode and grid portion of the tube. The area under the anode is 0.78" x 3.5", and this provides the necessary coupling with the chamber to develop the desired fields within the tube upon application of the RF drive pulse to the system. A tunable capacitance surrounds the anode feed shank; this sleeve can be moved to the appropriate position within the coaxial line formed by the anode feed and the grounded tube within which it is placed. The anode feed enters the chamber through a ceramic plate at the top of the anode feed; this plate provides both the vacuum seals and the high voltage insulation for the anode.

The grid of the tube is clamped to the flange which holds both the cathode and the anode feeds. The grid itself was initially made of tungsten wire 0.002" in diameter, spaced at 50 x 50 wires per inch. The grid-to-cathode spacing is 0.5 mm and the grid-to-anode spacing is approximately 6 mm.

Figure 2 RF Drive Block Diagram.

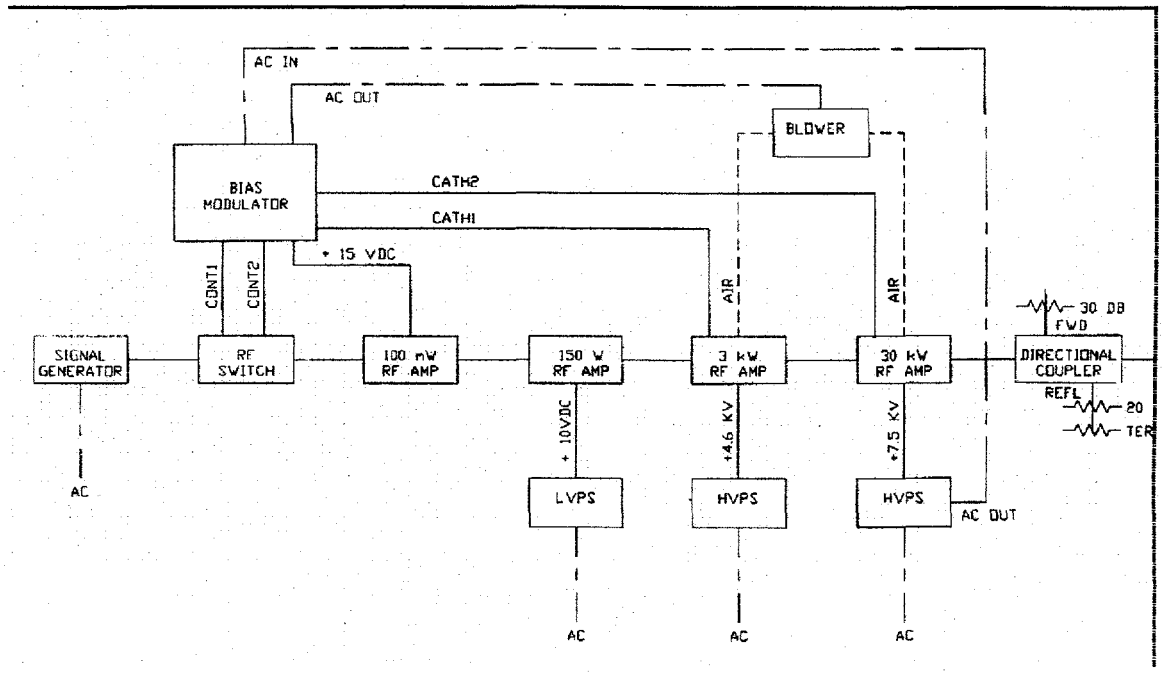

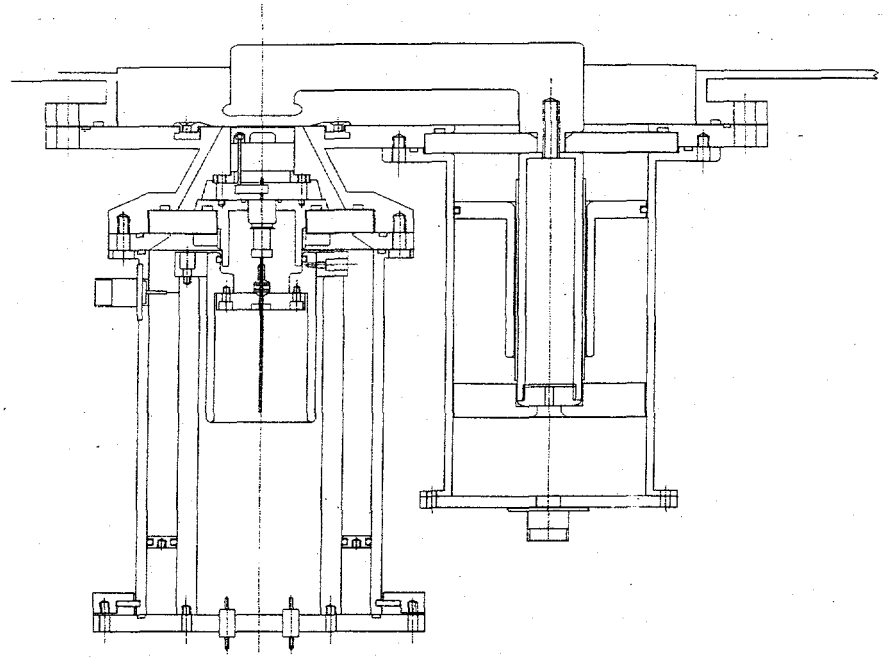

Figure 3 Medical waste tube attachment.

The cathode and its feed, seen on the left side of the figure, consists of a 1" dispenser cathode, "M" coated, mounted on standoffs to permit connections to be made from the cathode to the electrical feedthroughs into the vacuum region. As with the anode, the cathode system is both vacuum sealed and electrically isolated from the chamber by means of a ceramic disk. The cathode heater supply is a 24 V 12A filament transformer whose primary is supplied from a Variac, thus permitting the cathode voltage and temperature to be varied as required. A metal ring clamps the ceramic disk into position and permits the external part of the cathode feed to be removed and modified without breaking the vacuum seal. A metal sleeve is attached to the lower portion of the cathode body connection, outside the vacuum, and this sleeve forms one electrode of the capacitor used to couple RF energy into the cathode. A type N connector mounted on the outermost cathode housing provides the input point for RF to the outer electrode of the coupling capacitor. A sliding short between the outer electrode of the capacitor and the outer cathode housing permits tuning the cathode circuit. All metal-to-metal joints in the system have Tecknit knitted wire mesh RF gaskets between them in order to keep RF leakage to a minimum.

2.4 Vacuum System

The vacuum system consists of a Welch Duo-Seal Model 1402 mechanical roughing pump to evacuate the chamber via a 2" side port. Once the pressure is below about 100 microns, an Airco Temescal 6" gate valve attached to the external pumping tee is opened. This permits a Cryo-Torr 8 Cryopump to evacuate the chamber through the slotted electrode on that end of the chamber. The system routinely operates in the 10^{-8} range of pressure. The roughing vacuum is determined by means of a Granville-Phillips thermocouple gauge; the high vacuum is measured with a Granville-Phillips ionization gauge, which is capable of reading down to $1x10^{-8}$ torr.

2.5 Sensors

The cathode drive pulse can be measured by means of a Pearson current probe on the connection between the cathode pulser and the cathode; the cathode drive voltage is monitored with a scope probe at the cathode connection. The cathode heater voltage is continuously monitored with a Fluke AC voltmeter.

The anode voltage is continuously monitored with a North Star HV probe and a Fluke multimeter reading its 1:1000 output. The anode current pulse is monitored with a suitably insulated Pearson 0.1 ohm probe on the HV line between the anode supply capacitor and the anode.

The field in the cavity is monitored with an E-field sensor placed on the centerline of the chamber and even with the surface of the non-slotted electrode face. This probe measures the electric field at that point and its response is determined by its geometry. The probe consists of a length of RG-141 semi-rigid coaxial cable with one end connected via an SMA connector to an SMA vacuum feedthrough in a blankoff plate place at the end of

the central tube in one chamber electrode. The length of the coaxial cable is such that the end of the coax is even with the effective face of the electrode. The end of the coax is cut off square and cleanly so as to provide a well-controlled geometry for the electric field to produce a voltage on the center conductor. The voltage appearing on the center conductor follows the expression:

$$E = V/(50\omega\varepsilon A),$$

where V is the voltage measured on the coax,
ω is the radian frequency of the RF drive, about 1.885×10^{9}
ε is the permittivity of free space, 8.85×10^{-12} farads/m, and
A is the area of the center conductor of the coax, 6.567×10^{-7} m^2.

3.0 Operation of RF Accelerator 1

Once all the electronics are switched on and warmed up, the cathode heater is turned up to a level which will yield the desired level of current output. This is typically set to provide the heater with 150 watts or more of 60 Hz AC power. With the cathode at temperature and biased to a DC level of +100 volts, the anode is brought to its operating potential, typically 10 kV. The cathode pulser supply is raised to the level which will produce the current pulse needed from the cathode; the cathode pulse voltage is approximately 1/3 of the charge voltage of the cathode pulser. At this time the RF system can be set to deliver RF power to the cathode capacitive input connector and the various levels adjusted to yield the desired field level in the cavity.

3.1 Problems

Once the chamber had been copper-plated and all the parts were in, the system was assembled. The chamber was now cleaned thoroughly for vacuum service and the pumping system assembled and mounted to the chamber. The tube had not been assembled at that time, so a rectangular blankoff plate was put on the tube port for initial vacuum testing. The system was pumped down and allowed to clean itself up, reaching 5x10-8 torr within 2 days spent fixing minor problems and pumping.

With the chamber assembled, the RF drive tube was assembled with the cathode, grid, and anode, and all the associated hardware for those components. The tube assembly process took about one day, but much of that time was spent in organization. The chamber was then let up to atmospheric pressure, the blankoff plate removed and replaced with the tube flange, and the system pumped down once again. This time the pumping took somewhat longer, and the pressure did not fall into the 10^{-8} torr range until after the cathode had been degassed and run at high temperature for some time. The cold pressure of the system, however, did run as low as $4x10^{-8}$ torr once the cathode had been heated a few times.

Once the system had been assembled and the pressure was low enough, the cathode had to be activated. In order to do this, we raised the cathode temperature up to the point where the cathode bias pulses could cause the cathode to emit a reasonable electron current. By raising the cathode heater voltage up to as high as 20 volts, and driving the cathode to a pulsed bias level as low as -2000 volts, we were able to develop and reproduce adequate cathode emission current. For all this work the cathode pulses were 40 μsec long.

The RF system arrived tuned for 350 MHZ; when we tried to tune it for 300 MHZ, it could not deliver the 40 μsec rectangular pulse. The pulse available at the output of the 150 W amplifier is roughly triangular, and no more than 5 μsec at FWHM. A replacement 150 w amplifier has been ordered, but work is proceeding using this pulse until it arrives. In the absence of a 40 μsec pulse from this amplifier, we cannot tell whether the 3 kW and the 30 kW amplifiers will deliver the full pulse width at 300 MHZ. However, even with this short pulse, we attained a field of 1.3 MV/m in the cavity.

After some period of testing, we noted that the cathode current gradually fell off from its initial level over a period of several minutes. We were able to regain the previous level, but only by increasing the drive level, the cathode temperature, or both. When we spoke to the manufacturer of the cathode and described our setup, we were told that we had almost certainly poisoned the cathode to some degree with vaporized gold from the gold braze used to secure the grid mesh to the grid support spider. We removed the brazed grid assembly and replaced it with a simple mesh of molybdenum wire with no additional support or heat conductors, and tried the cathode drive again. It seemed that there was some residual poisoning of the cathode, shown by a reduced current output level.

Fearing that the once-poisoned cathode would never truly recover, we replaced it with an identical spare cathode, taking the opportunity to inspect the parts and the surrounding area for damage or overheating. While there was plenty of evidence of heating, there is no reason to believe that any component or structure in the area was overheated during operation.

We got more output from the new cathode, and then added a cathode field sensor to enable us to determine the cathode voltage and waveform directly. This sensor was made from an ISI SMB DelWeld adapter, welded into the shell surrounding the cathode. This sensor resembles the other electric field sensor used to measure the electric field in the chamber. Our experiments then were hindered by frequent cathode to grid shorting when the cathode was hot.

We shimmed the grid in order to place it further from the cathode, but it still shorted the cathode when the cathode was near operating temperature. We increased the cathode to grid distance to about 1 mm, and were then able to operate without cathode shorting. At that point we calibrated the cathode electric field sensor, and determined that it read 1:1674 volts of the cathode voltage when terminated in 1 MΩ.

We measured the maximum current available from the cathode when driven by a negative pulse for various cathode heating voltages, and found that we could not get enough cathode drive for our purposes; the drive level was well below that predicted by the Child-Langmuir Law. Thinking that we might not be getting enough heating for the (unprotected) cathode to emit properly, we fabricated a two-layer heat shield from .003" thick Ta, and tried the cathode. This cathode was apparently worse with the heat shield on it, so we fabricated a new two-layer heat shield from .001" Mo and put that on the refurbished cathode and installed it. We tried running that setup up to full heat, but once

again shorted the cathode to the grid. We removed the grid spacers and installed a new grid spaced 0.5 mm from the upper surface of the cathode. We also started looking into coating our own cathodes with electron-emitting material.

With the new setup, after regenerating the cryopump and baking the entire system under vacuum to clean it up as much as possible, we were able to get 30A from this cathode setup with 20.5 VAC for cathode heating and pulsing it to about -1200V. The next day (8/2/95), while preparing to run with RF drive, the cathode once again was shorting to the grid when heated up to nearly its operating temperature. We decided to investigate coating our own cathode with a mixture of barium carbonates, but, once we got more data, this did not seem like a worthwhile idea. We also decided that we needed to find a better grid; one that would not bend so much when heated to the needed operating temperature.

4.0 Operation of RF Accelerator II

4.1 Differences from Accelerator I

The second RF accelerator design concept is essentially the same as the first, but there are some significant differences. The second design has only one separable joint in the main current path inside the accelerator: the two electrodes and one end flange are welded to the main chamber. The other end flange joint is the same as that for both end flanges in the first design. This change was instituted to reduce the resistance to electron flow in chamber walls. Secondly, there are two series chambers in the second design, rather than one. This is to increase the beam voltage. The third change is that the electron "tube" in the chamber is scaled up over the first by a factor of two in size in order to increase the current-carrying capabilities of the device.

4.2 Chamber

The two RF Accelerator chambers for the second design are identical. They are about 17-3/4" long and 16" in diameter. The inside dimensions are 15.721" in diameter and 17.323" in length. The two electrodes are 6" in diameter and have a face-to-face spacing of 5.27". These dimensions yield a resonant frequency of about 300 MHZ. The inside of both chambers is plated with 0.002" thickness of bright acid dip copper. The rectangular port for the tube is 11.5" x 4.5", and the area under the anode is 5.25" x 0.77". Each chamber has three NW50 nipples in a row opposite the rectangular tube opening. The two chambers are both bolted to a vacuum tee at the slotted electrode pumping port, and they are both pumped by means of this tee. The same vacuum system is used for this part of the experiment as was used for the first chamber.

Measurements made on these chambers yielded Q values of about 6000 at best. Several measurements were made in an effort to determine where the losses were, and the conclusion was that, at the vacuum joint where the NW500 flange is clamped to the chamber, the o-ring support ring was not making good enough contact. We fabricated a circular ring of annealed copper tubing, with the ends soldered together over a central piece of copper wire, and put that in place between the flange faces and clamped the flanges together just enough to permit centering the ring and holding it in place. We then placed a 1/4" cross-section o-ring around the copper tubing ring and clamped the flanges together as tightly as the 17 claw clamps would permit. The measured Q after this was accomplished was 12,183, well within the design goal. The data for these determinations are plotted in Figures 4A and 4B.

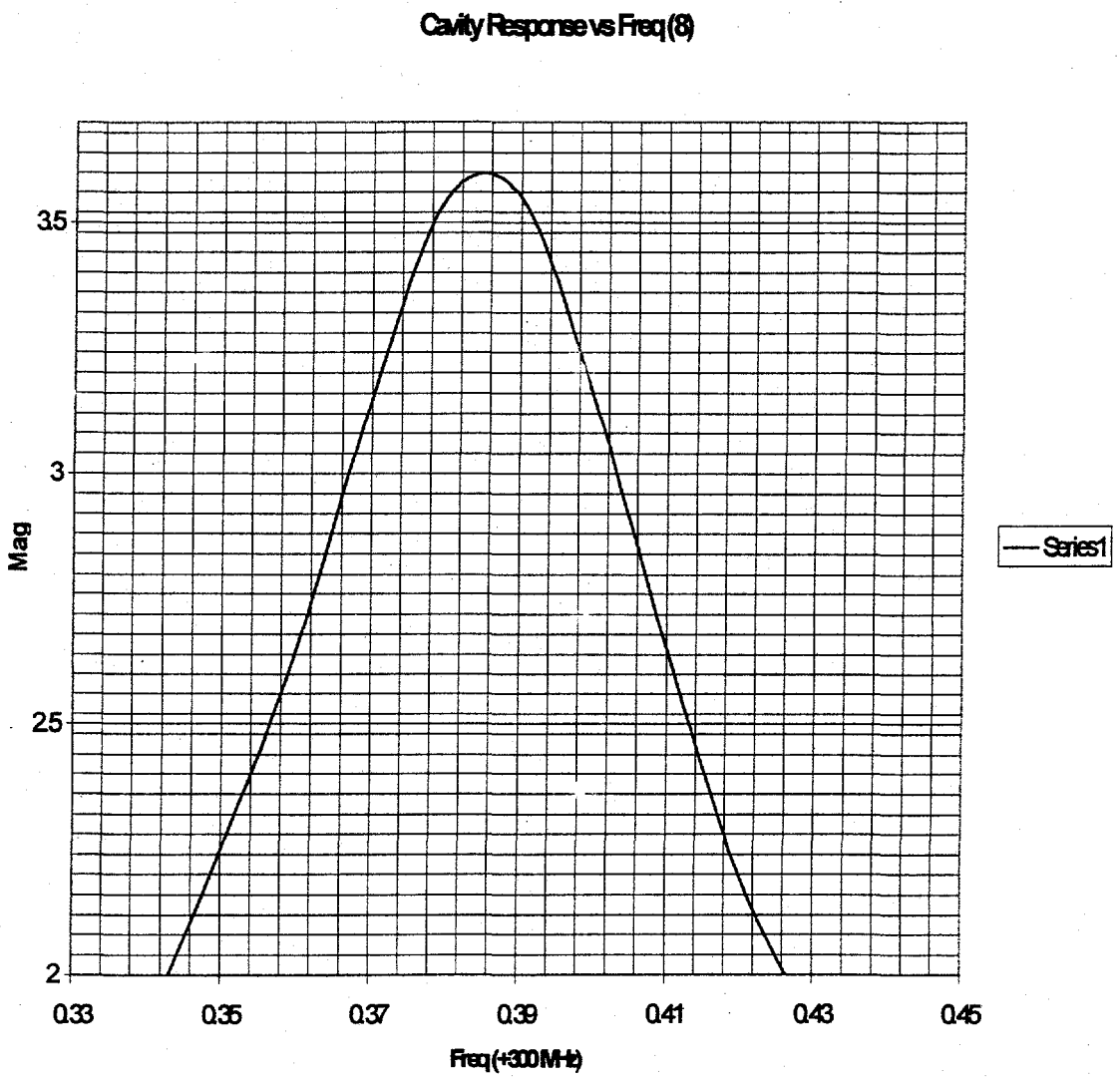

Figure 4 Measured Q.

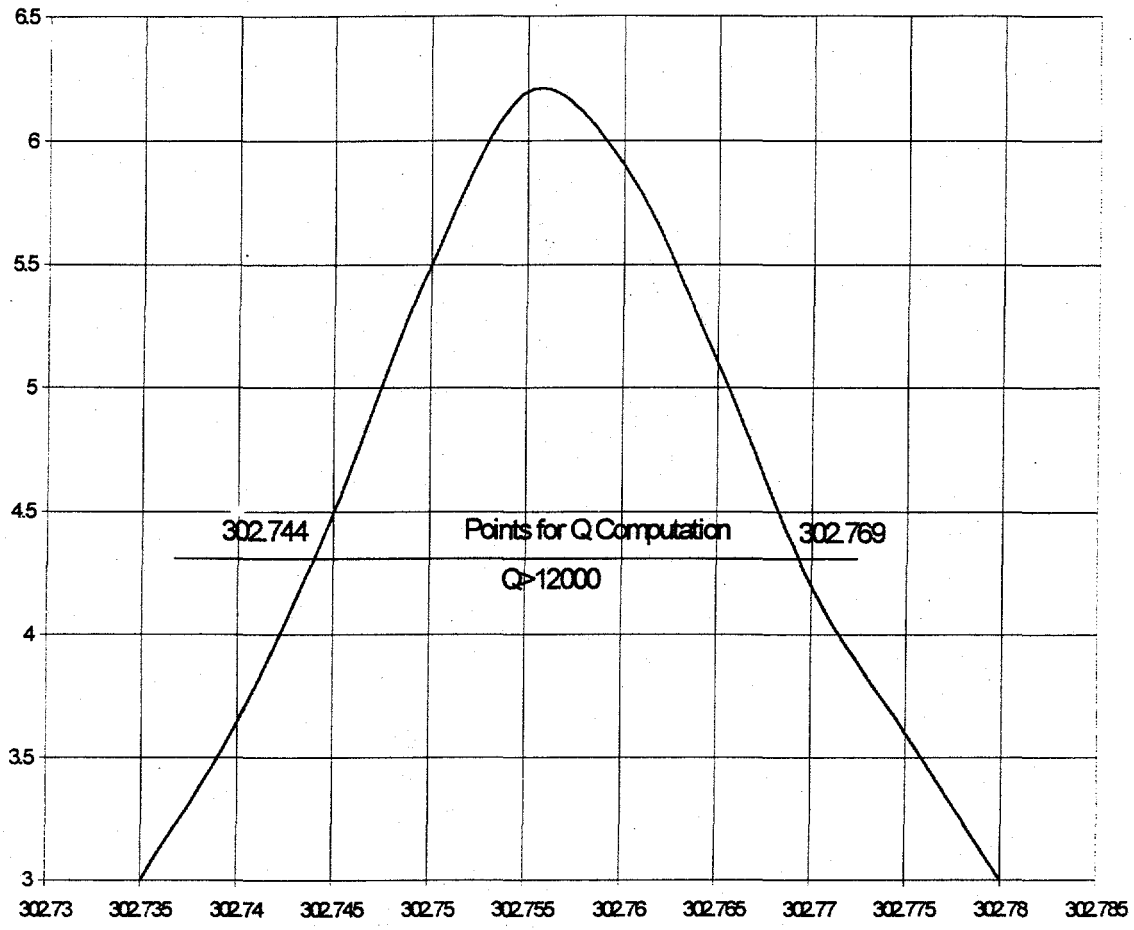

Figure 4b Q plot after adding the copper gasket showing improved Q.

The 2" cathode used in these tubes is rated to reach 1100° C at 20.1 V and 16.87 A. We ordered an additional filament transformer to parallel with the existing one in order to have enough power to run this cathode properly. We chose to start with a simple grid made of 20x20x0.005" W wire with the minimum spacing possible between the grid and the cathode: 0.013". Our initial run with this setup showed that the grid was shorting the cathode when heated. We added 0.020" shims between the grid and the cathode and tried that spacing. The grid still shorted the cathode to ground. Just in case we were mistaken about the mechanism of the short, we tried heating the cathode with no grid in place. This diode did not show any signs of shorting the cathode to ground.

Next we tried a new grid, made of 20x20x0.005" W, spaced at 0.062" from the face of the cathode. This setup shorted out the cathode at only 8.5 VAC on the cathode. We noted that the nature of the grid is such that, on cutting a circle from the roll of material, the cut grid sometimes resembles a potato chip. We tried to prevent this poor grid shaping by clamping the grid material flat between plates before cutting it under that constraint. On heating, this grid shorted to the cathode at about 9 VAC on the cathode. We spent considerable time trying to devise a method of pretensioning a grid so as to maintain flatness under heating. The next idea we tried was to support the grid by a few tungsten rods held only at one end, so that they were free to expand lengthwise with no obvious reason for bowing. We built a grid assembly with three 0.020" diameter tungsten wires, one going all the way across the grid and each of the other two coming in at right angles to the crossing rod but not quite reaching it. Figure 5 shows a photograph of this grid clamp and rod structure.

This new arrangement seemed to be successful at preventing cathode shorting. At 20.4 VAC on the cathode, with +300V cathode bias and pulsed drive of approximately -500 volts reached, the cathode emitted 19A. With the anode at 8000V and the cathode driven hard, it was able to emit over 100A. The next time the system was run, the maximum current available from the cathode was 10A when driving it quite hard.

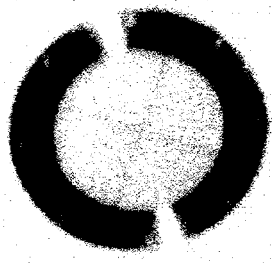

Figure 5 Grid clamp structure

When the system was next run, we were able to get about 22 A drive from the cathode with 21.5 VAC on cathode, driven with 4000 volts on the cathode pulser and the anode at 4600 V. We then applied RF to the system and got some RF in the cavity. We could not tell if we were getting amplification at that time. The grid has to be closer to the cathode in order to improve the gain of the tube. With that in mind, I made a tool to produce some shims for spacing the grid differently. The anode to cathode spacing is about 0.155". If the grid material is 16x16x.008" Mo, the grid thickness is about 0.016". With the grid spaced 0.020" from the cathode, the upper surface of the grid will be about 0.130" from the anode. The current placement of the grid was determined to have the lower surface of the grid about 0.052" above the cathode surface. This grid arrangement is about 0.035" thick, due to the thickness of the 0.020" tungsten rods adding to the grid material thickness. Hence the grid to anode spacing was about 0.063". We removed 0.020" of shims, moving the grid 0.020" closer to the cathode. With the cathode strongly heated (after degassing and conditioning), we were able to obtain about 26A emission from the cathode. We decided that it was probably not necessary to apply a rectangular pulse to the cathode in addition to the RF signal; the class C amplifier should amplify the RF even if no additional pulse is applied. We ran the system this way and got increasing field in the chamber with increasing RF drive, as one would expect. In addition, increasing the anode voltage increased the magnitude of the RF signal in the chamber for any given RF drive level. The next day, trying to replicate these results, the cathode shorted to the grid at the operating level used before.

We opened the system and installed an additional shim (0.010") to increase the grid to cathode distance and attempt to end the cathode shorting. Initially we were able to run the cathode up to its operating level and pulse it with the cathode drive. This was successful, but when we started applying RF to the cathode, it started breaking down to the grid. After a few such breakdowns, the cathode would not hold a DC level any higher than 60 V.

We then removed the existing grid setup and installed a completely different one. This arrangement has a free-floating tungsten grid made from 16x16x0.008" material, spaced about 0.042" from the surface of the cathode. The round grid is free to move laterally, but is held captive by the shims and the upper grid clamp. It is hoped that this system will permit the grid material to expand without causing such a departure from planarity. After bringing the pressure in the system down, and outgassing the cathode for a while, it was possible to run the cathode drive up to 23.2 VAC and get more than 15 A of emission from it. We then ran the system with RF and with no other cathode pulsing and were able to see RF in the tank. The cathode was not shorting out, but the tube did not seem to show any gain. In addition, the RF level does not seem to show the sharp peak with tuning that it showed earlier when the RF level in the tank was much higher.

We ran the system the next day, and were able to drive the cathode to give about 17.5A. We then started to apply RF with the cathode biased to +200V but without the cathode pulse. At 302.27 MHZ, we got up to 1.4 V peak to peak from the field sensor, with the anode at 6200 V. Turning off the anode voltage caused the field sensor output to drop to about 50% of its previous level. At the same time the anode voltage went to

about -110V. A reading of 1.4 V peak-to-peak from the field sensor corresponds to a peak field at the sensor of 0.7/5.54E-7 = 1.28 MV/m. This level, with the distance between the electrodes of 20 cm corresponds to an accelerating voltage of 260 kV.

4.3 Conclusions on RF Accelerator 2

Further studies suggested that multipactoring prevented voltages above those observed above. During some pulses, 500 kV (>2.5 MV/m) was observed. We were unable to prevent multipactor breakdown even with the application of more rapid risetimes. The voltage per cell was found to be limited in all cases to 500 kV. Although we had two cells available, we did not have sufficient power to drive both cells. The single cell voltage level was insufficient to perform any irradiation work on the contract.

5.0 Performance and Testing of the Irradiation Concept with a DC Accelerator

During the performance of the work described above, it became clear that the accelerator concept was sound in principle, but that the details of fixing the grids, etc. would prevent us from completing the project within the budget. At the same time, we found a vendor (the American Pulverizor Company) capable of shredding and decreasing the diameter of the material better than we previously thought possible. This in turn allowed us to consider lower energy irradiation of the waste. This thinner waste allowed us to perform irradiation at energies between 650 and 850 kV. The thinner waste as used in this project is shown in Figure 6.

Figure 6 Waste from American Pulverizer compared to a human hand.

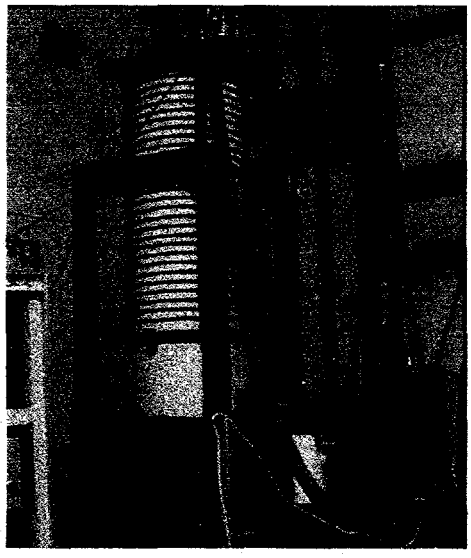

Figure 7 Nested High Voltage DC Accelerator.

The DC accelerator used was a Nested High Voltage Generator (NHVG) built by North Star for another project. This device produced a beam of current 100 - 300 uA during our medical waste irradiation studies. This device is shown in Figure 7. For future use, the NHVG is capable of operating at up to 1 mA and 1 MeV. It has fully solid state power drive, and it does not make use of any greenhouse gases such as Sulphur Hexafluoride for operation.

5.1 Medical Waste Irradiation Setup

Side views of the waste irradiation setup are shown in Figures 8 and 9. In Figure 8, we can follow the beam down from the machine into the scan chamber. In that view, the

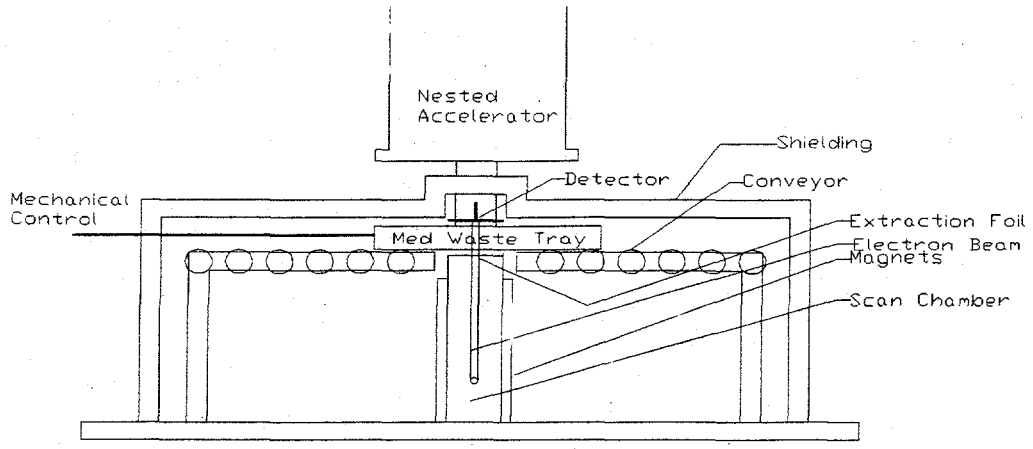

Figure 8 Medical waste system side 1 view.

beam goes down, and is scanned "out of the page" towards the viewer. The medical waste on the medical waste tray (see Figure 10) moves from left to right using a hand or motor driven mechanical control. Shielding surrounds the setup for personnel safety. One of the advantages of this setup is that the shielding need not be thicker than 2" of lead.

Figure 9 gives a better view of the electron orbits, in the scan chamber. A set of 6 sequentially timed magnets moves the electrons from the left to right in a controlled "scan". The length of the scan used in this work was approximately 14 inches.

The collector shown in Figures 8 and 9 provides a measurement of the current which transmits through the medical waste. An investigation of that technique for determining penetration of the waste was one of the main goals of the project.

We investigated the penetration using two techniques shown in Figure 10 - the step wedge of aluminum foil, and the impenetrable wedge of aluminum sheet. The tray has a 25 micron thick stainless foil which lets the beam penetrate with low loss, but with some scattering.

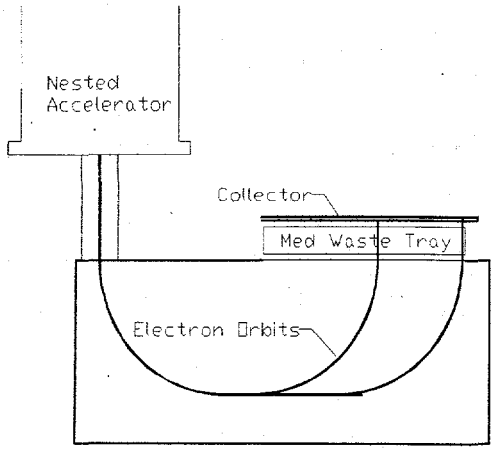

Figure 9 Medical Waste Beam side View.

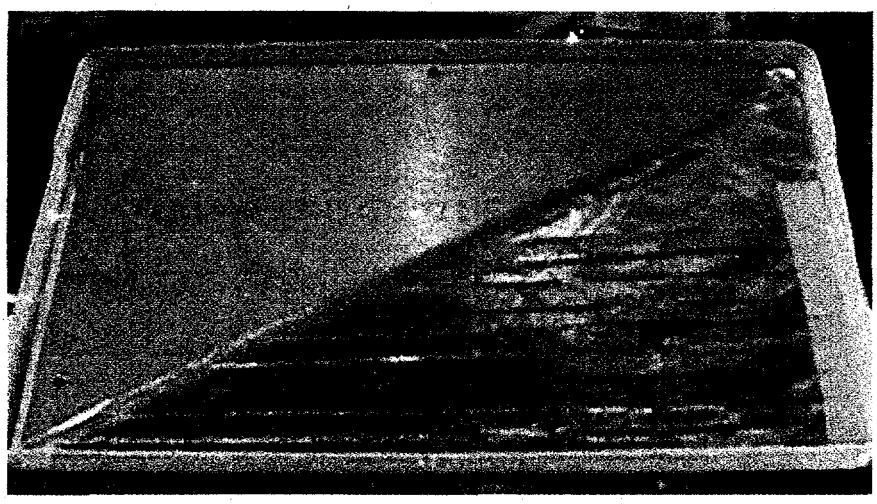

Figure 10 Tray showing impenetrable sheet, and step wedge of aluminum foil.

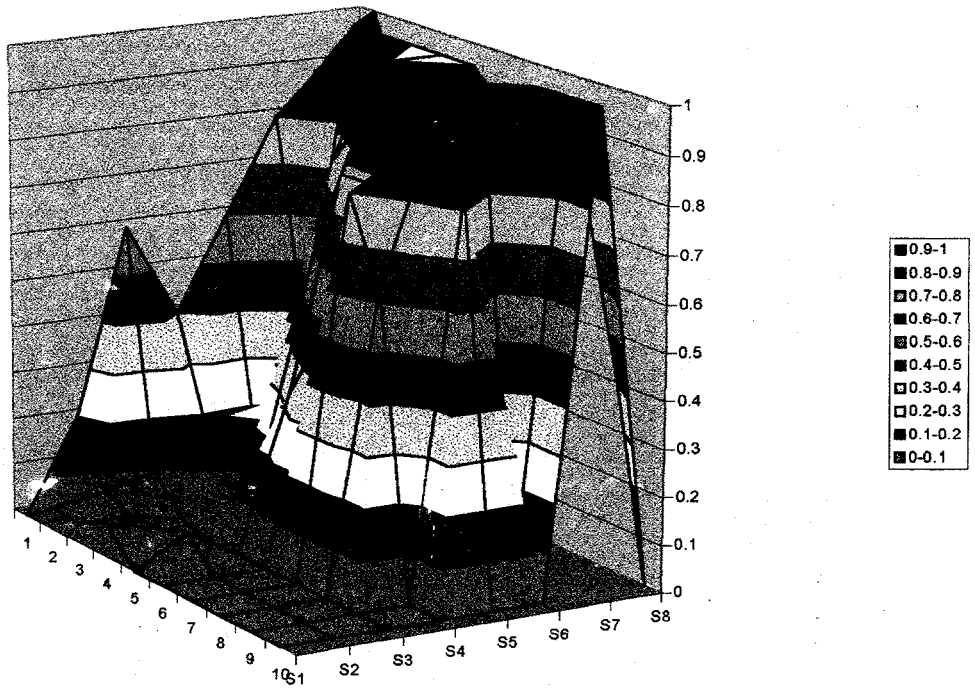

Figure 11 Medical waste data normalized for the triangular wedge case.

5.2 Results

Several tests were performed with the medical waste and various simulations of the waste. We first placed 20 grams of waste on the tray and irradiated it. Using radiochromic film we found that the waste was completely penetrated by the electron beam. This is expected because the amount of waste (20 grams/900 cm^2 = .022 g/cm^2) is expected to be easily penetrated at 750 kV - the typical electron energy. The typical penetration is 0.28 g/cm^2 at 750 kV, and we observed that the waste placed in the tray was uniformly irradiated.

The critical question is whether waste which isn't penetrated by the electron beam can be irradiated or rejected for alternate processing. The technique originally proposed was the detection of the electrons after transmission through the waste. We tested this method of detection using the triangular impenetrable wedge shown in figure 10. The data from the wedge experiment from one of the two collectors is shown in Figure 11. In Figure 11, we show the relative flux at each time point during the scan. The data can be seen to have a roughly triangular outline. The half value point with the edges ignored is plotted against the actual wedge position in Figure 12. In Figure 12, the location of the edge of the wedge is found to be acceptable, indicating that gross objects can be "imaged" by the penetration of the electron beam. Unfortunately, the resolution of this "image"is about 1 inch which is not a fine enough resolution to reject unirradiated material.

We verified that a 1" wide object could not be imaged by this technique by attempting to image a steel rule. The change in the X-ray flux was also not measurable in the background due to the collector.

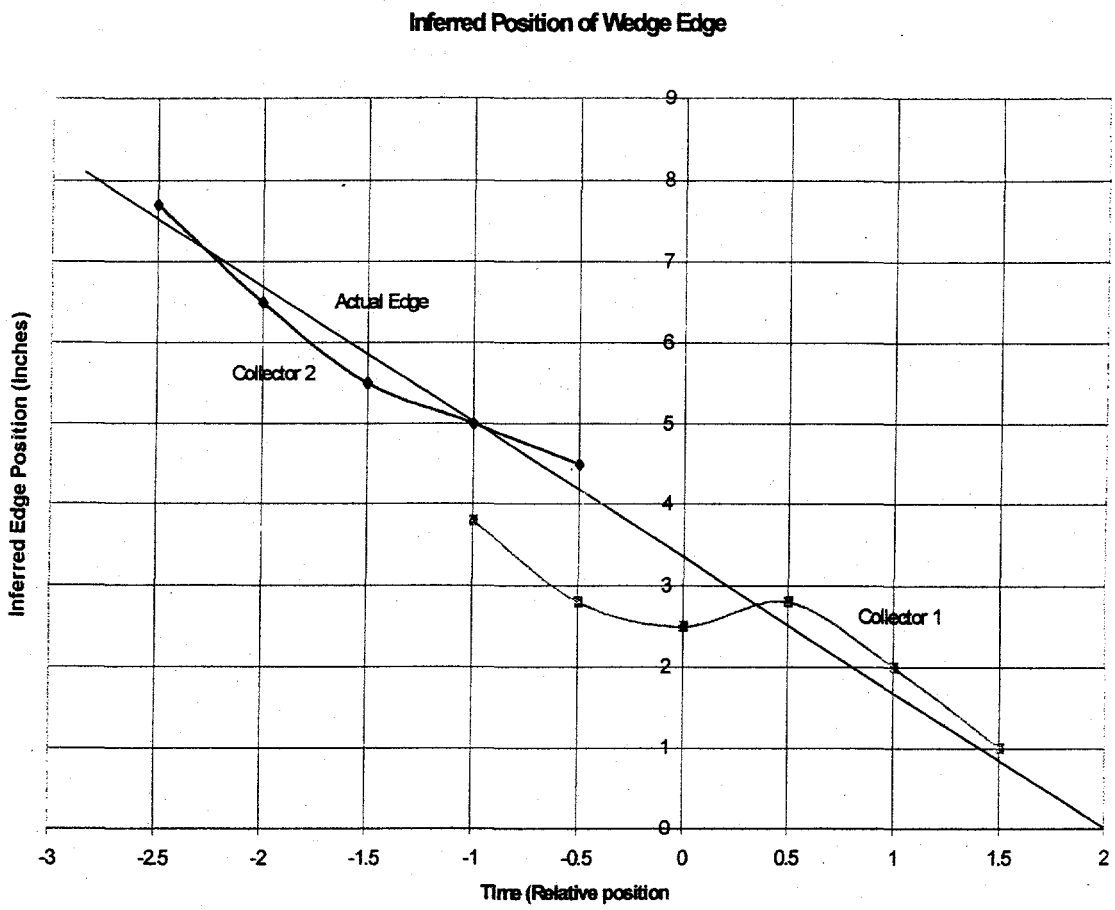

Figure 12 Inferred and real edge position.

We observed the penetration for the beam through various calibrated thicknesses of foil, and found that it was in excellent agreement with the expectation from Cyltran runs.

There is some hope that the resolution would improve if the energy were higher, but unfortunately, the distance which the beam would economically be required to penetrate would also increase.

We therefore conclude from this work that for plastic and cloth based medical waste the method used is successful and effective. It is not capable of distinguishing the presence of impenetrable objects such as metals to a degree of accuracy which we deem to be acceptable.

6.0 Scaling to Facility Size

The clear effectiveness of hammermills combined with shredders opens up new opportunities in medical waste handling. This means that most of the waste can be "thinned" to the point where a 1 MeV beam will successfully irradiate it. We have demonstrated that capability in this work. The remaining issue is the effectiveness of a cost-effective technique for detecting and treating those parts of the waste stream which are not readily thinned by the hammermill. We note that multiple passes with a hammermill are possible, and that gravity separation of the waste is a practical possibility.

6.1 X-ray Backscatter Detection of Thick Waste

An X-ray backscattering system could be used to provide a precise measure of the thickness of the material. When an X-ray at medium (say 80 kV) energy strikes a target, there is a significant probability that the X-ray will be reflected via "Compton Scattering"[1]. In the Compton process, the probability of a scatter event depends on the number of electrons in the path. Electron range also depends on the number of electrons in the path, so this provides us with a direct measure of the electron range before irradiation. If the tray contains material which is too thick to irradiate, the waste will be returned to the hammermill and then re-processed. Validation of the detection technique becomes the major issue in low energy irradiation since the effect of electron irradiation on pathogens is well established.

A sketch of an X-ray backscatter system is shown in Figure 13. It consists of a standard (say 120 kV) X-ray tube, a large area detector, and a photomultiplier. The mechanical scanning of the X-ray beam provides the requisite resolution. The presence of chlorine (from PVC) provides some attenuation of the scattered X-rays, but we reduce this effect by "hardening" the spectrum using a steel absorber on the surface. Low energy photons are rejected by this technique.

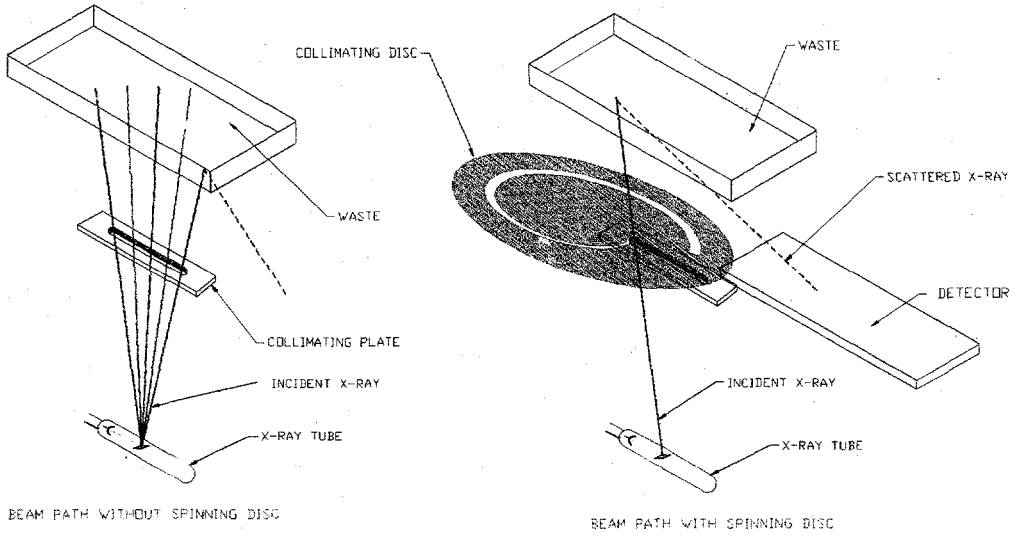

Figure 13 X-ray backscatter concept for medical waste thickness measurement. The spinning collimating disk, when combined with the collimating plate, produces an X-ray pencil beam which is scattered to a degree determined by the thickness of the material.

6.2 Nested Generator Design For Waste Irradiation

Our Nested Generator Technology[2] provides a cost effective means of generating beams in the 0.3 - 2 MeV range. The technique uses a set of series voltage multipliers encased in a combined oil/plastic dielectric to hold voltage gradients.

The primary motivation for the development of the NHVG was the requirement to significantly reduce the size of a DC accelerator, and the primary means of reducing the size was to use solid insulation in order to decrease the diameter of the machine. The fundamental problem of solid insulation is that as the voltage increases, the allowable electric field for insulation drops.

The NHV concept is that the only way that the voltage can be subdivided uniformly without voltage concentration in a fault mode is to split the high voltage structure into nested Faraday Cages in which each one has its own power source. The power is supplied to the Faraday cages by allowing azimuthal electric fields (axial magnetic fields) into the individual cages. In this embodiment, the NHVG is a distributed air core switching transformer with each coil/power supply coupled to its own insulation.

An intrinsic advantage of the NHVG relative to other DC generators is the way that the segmented voltage system affects the behavior of the system components in case of a fault mode as shown in Figure 14. Because each vacuum interface (hatched element in the figure) is associated with its own capacitance, and there is no other total system capacitance, the voltage in a fault does not exceed the ambient voltage. In DC accelerators, spark gaps are placed along the column to prevent voltage transients from building up, but even with spark gaps, components are subjected to 3 times the ambient voltage because the pulsed hold-off voltage of the spark gap is typically 3 times the DC hold-off voltage.

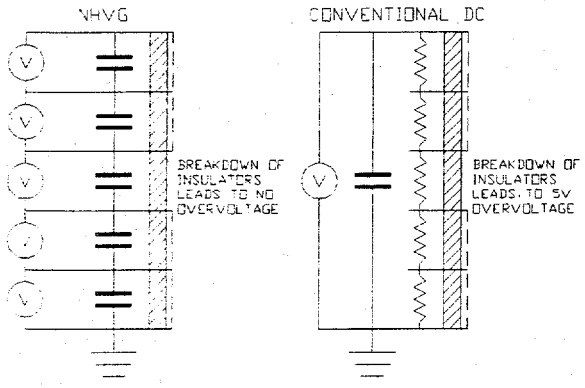

Figure 14 Nested High Voltage and DC accelerators in a fault mode. The NHVG fault mode voltage does not exceed the operating voltage. The DC accelerator is subject to extreme over-voltage.

The most common machine fault modes involve flashover along the insulators, and we have designed the accelerator with resistance between the nested conductors and the associated vacuum electrode. This means that almost all of the stored energy is dissipated in resistors in the case of a fault.

A typical cross-section of an NHVG is shown in Figure 15. Insulation is provided in the radial direction by multiple layers of high dielectric strength film, and in the axial direction by a combination of plastic film or sheet, and dielectric

fluid (oil). All films are impregnated with thin layers of this fluid. The potentials of each stage are defined by axial, cylindrical, conducting metal sheets which form the outer and inner boundary of each stage. These sheets are terminated on the ends by spiral conductors which are used to connect the grading rings on the insulator stack to the cylindrical metal sheets. No electrical connections are made between stages except by the conducting sheets.

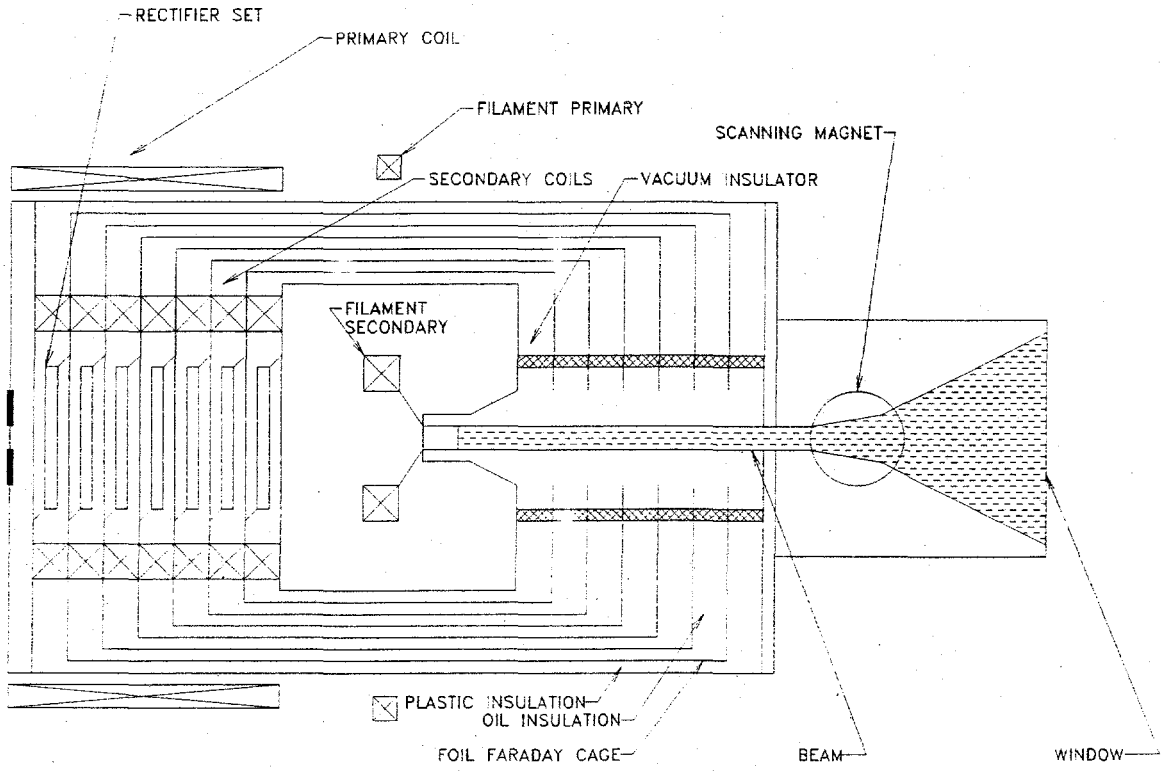

Figure 15 Nested Generator typical setup.

6.3 Physical Parameters of a Complete System

A waste handling system at an operating energy of 1 MeV will have the capability of penetrating 2.5 mm of solid plastic material. Given the density of the pulverized waste, this unit will have a tray which is approximately 2 inches deep. Planning for a net thickness equivalent to 1.0 mm of material, and a scanning width of 40 cm, the average weight of a 40 cm long tray will be 160 grams. We believe that such a system should process at least 5,000 lbs/day to 4 Megarads, so we need a conveyor system capable of moving 15,000 waste shuttles per day over a 14 hour day (about 3 seconds per shuttle). This corresponds to a speed of 13 cm/second - a modest speed for such a system, but one which still must be considered in the design. The power required to reach the 4 Mrads sterilization level is inferred by noting that the conversion is 10 J/g/MR. All waste must be exposed to 40 J/g, and each shuttle, if filled full range would have 1600 cm^2 X0.3 g/cm^2, or 500 grams. This corre ponds to a power level of 7 kW. This level is twice as high as we have previously operated the accelerator.

We summarize the proposed parameters:

Waste sterilized	5000 lbs/day
Shuttle area	40 cm X 40 cm
Conveyor speed	13 cm/sec
Dose	4 Mrads
Beam Power	7 kW
Beam Power in Waste	2.5 kW

6.4 Ultimate Cost

The major capital cost items are the accelerator, conveyor, pulverizor, and screening X-ray system. A diagram of this is shown in Figure 15.

We have built a 1 MeV machine which, in its second iteration, can be built for the following costs. The critical scaling from the existing 1 kW machine is the scaling from 4 to 12 modulators.

Nested Generator - Modulator	12	6k	72
Nested Generator - Structure	30	.2	12
Nested Generator - Cells	30	500	15
Nested Generator - Housing	1	4	4
Nested Generator - Mylar/Copper	800	8	6.4
Nested Generator - Labor	1000	35	35
Misc./Controls	1	15	15
Vacuum System	1	18	18
Cathode System	1	6	6
Total			180

Pulverizer/shredder				20	
Conveyors				9	
Scanner Chamber			4		
Scanner Magnets	6	.5	3		
Scanner Electronics	6	.6	3		
Total Scanner				10	
Housing				15	
X-ray Power Supply			5		
X-ray tube			2		
Scintillator/mt			2		
Structures			5		
Control Computer/Data Acquisition				6	
Other Labor	500	40		20	
Total				260k	
Cost of Sales				50	
Total					310k

Conveyors

Standard conveyors would be used as sold by a variety of organizations.

X-Ray system for Pre-Scan

North Star can use either a separate system (as depicted in the system diagram of Figure 15), or its MeVScan technology which uses the initial system requiring 5 scans per second of X-ray data.

Scan Chamber

The scan chamber should be similar to that used by NSRC in the present work.

Assuming a 5 year amortization of the cost, and 2 shifts of operation, the basic labor and equipment cost of a system such as the one we are studying is approximately $150,000/yr.

Under the assumption of 5000 lbs/day, the net cost of irradiation is $150,000/(365 X 5000 lbs) = $.083/lb.

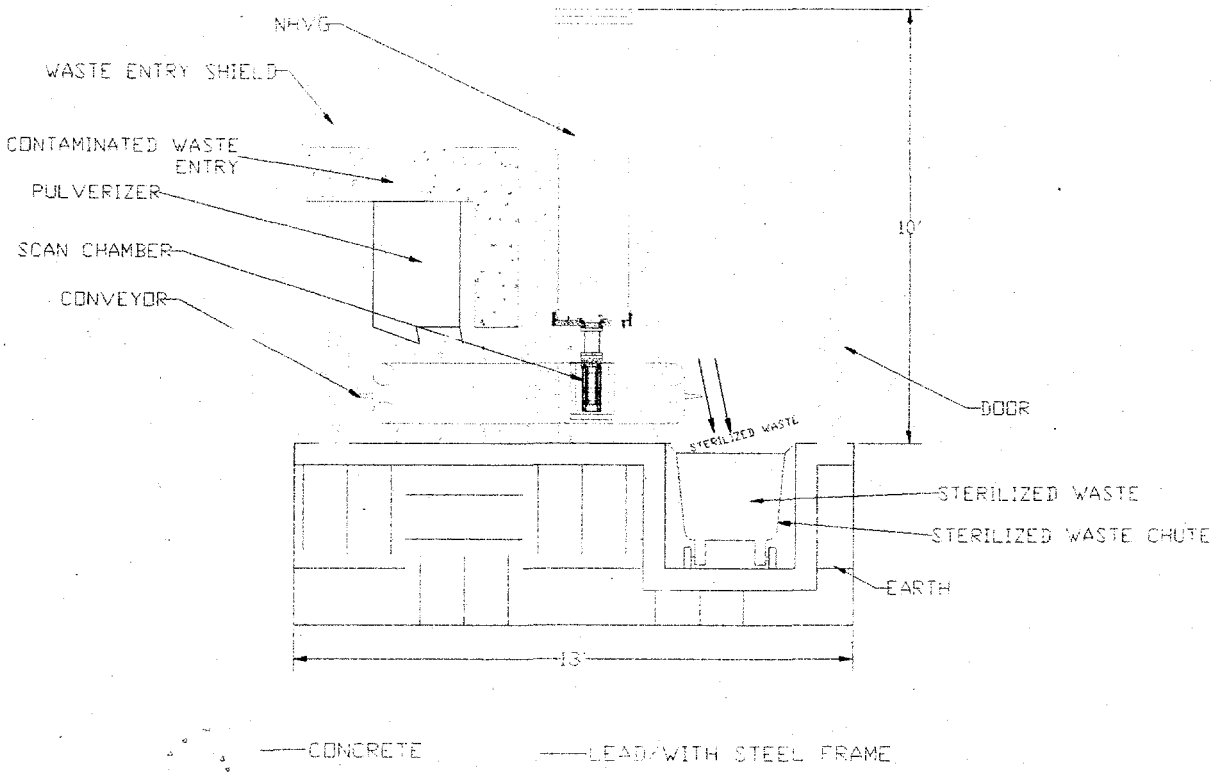

7.0 Conclusions

We have performed an ambitious study and experimental study of simulated medical waste irradiation with low energy (1 MeV) electron beams. We have also attempted with modest but insufficient success, to develop an extremely low cost accelerator module for medical waste irradiation. The conclusion of our study are:

The tube accelerator module will take more work to become operational, but it's energy is not necessary for economic electron irradiation of waste.

Low energy irradiation combined with state-of-the-art pulverizing technology is a feasible, cost effective technique for medical waste irradiation

X-ray scanning of the waste to eliminated large or dense pieces can be performed in order to prevent irradiation of overly thick waste.

1. See, for example, Henry Semat, "Introduction to Atomic and Nuclear Physics" Rinehart, New York, 3rd edition, 1954 p. 160.

2. R. J. Adler et. al. In "Novel Applications of Lasers and Pulsed Power" SPIE proceedings Volume 2374, p. 194, 1995.